Force-mediated molecule release from double network hydrogels

Article *in* Chemical Communications · September 2021

DOI: 10.1039/D1CC02726C

8 authors, including:

Yuwan Huang
UNSW Sydney
2 PUBLICATIONS **7** CITATIONS
SEE PROFILE

Jamie J Kruzic
University of New South Wales (UNSW Sydney)
209 PUBLICATIONS **6,007** CITATIONS
SEE PROFILE

Kristopher Kilian
UNSW Sydney
89 PUBLICATIONS **5,348** CITATIONS
SEE PROFILE

Force-mediated molecule release from double network hydrogels

Pavithra Bhakthi Jayathilaka, [a] Thomas Gregory Molley, [b] Yuwan Huang, [c] Md Shariful Islam,[b] Michael Robert Buche, [d] Meredith Silberstein, [d] Jamie Joseph Kruzic, [c] and Kristopher Alan Kilian *[a,b]

[a.] School of Chemistry, University of New South Wales (UNSW Sydney), Sydney NSW 2052, Australia
[b.] School of Materials Science, University of New South Wales (UNSW Sydney), Sydney NSW 2052, Australia
[c.] School of Mechanical and Manufacturing Engineering, University of New South Wales (UNSW Sydney), Sydney NSW 2052, Australia
[d.] Sibley School of Mechanical and Aerospace Engineering, Cornell University, Ithaca, NY, USA
* E-mail: k.kilian@unsw.edu.au

The incorporation of mechanosensitive linkages into polymers has led to materials with dynamic force responsivity. Here we report oxanorbornadiene cross-linked double network hydrogels that release molecules through a force-mediated retro Diels-Alder reaction. The molecular design and tough double network of polyacrylamide and alginate promote significantly higher activation at substantially less force than pure polymer systems. Activation at physiologically relevant forces provides scope for instilling dynamic mechanochemical behavior in soft biological materials.

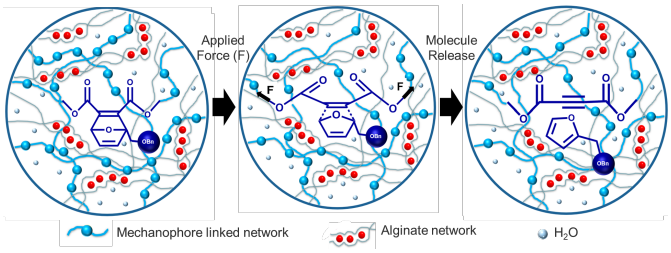

Fig. 1 Synthetic approach for generating the mechanophore crosslinker and scheme for mechanochemical activation and molecule release in double network hydrogels.

Mechanochemistry, the study of how applied force facilitates chemical transformations, has gained considerable attention recently in polymer systems.[1, 2] The concept of mechanochemistry was first introduced to polymers by Staudinger in the 1930s.[3] Since then, polymer mechanochemistry advancements have grown into exciting areas such as catalysis, self-healing, drug delivery, and sensory materials.[4] This research has expanded in two primary directions: designing novel mechanophores, and developing new materials incorporating mechanophores.[5, 6] The principle of mechano-responsive materials is based on integrating molecues with force responsive bonds (mechanophores) into polymer backbones or within crosslinkers.[1] For example, spyropyran,[7, 8] 1,2-dioxetane,[9] β-Lactam,[10] cyano-substituted cyclobutene,[11] dithiomaleimide,[12] rotaxane[13] and gem-dihalocyclopropane.[14] have been widely used as mechanophores or multi-mechanophore systems.[15] These mechano-responsive polymers are attractive due to their ability to produce signals for sensing damage, for the improvement of mechanical properties (e.g., self-healing), and for the release of small molecules with a con-current signal or radical/catalyst generation,.[16, 17]

All early reports of polymer mechanochemistry employ pure polymer systems or mechanophore immobilization at the interface of hard materials.[18-20] Seminal work by Moore, Sottos, White, and colleagues introduced a polymeric material consisting of a spyropyran ring structure that transformed into the merocyanine form in response to force with an associated color change.[21] Since then, many groups have reported unique mechanochemical systems for mechanochromic and mechanoluminescence force sensors,[9, 22, 23] as well as 3D printing,[24] the activation of mechano-catalysis,[25, 26] materials with self-reinforcing/self-recovery properties,[27] revealing new functional groups,[28, 29] mechanically triggered polymer degradation,[30] and small-molecule release.[31, 32] Despite these advances in the area of polymer mechanochemistry, integration of mechanophores within hydrogels has remained relatively unexplored.[33, 34] This is largely because most mechanophore systems are hydrophobic molecules that cannot be integrated with aqueous systems. Furthermore, hydrogel materials are often brittle and unable to withstand the applied forces necessary for activation.[35, 36] Therefore, studies on hydrogel mechanochemistry have mostly been based on fluoresce/color changes[37] or radical generation.[38]

Here we demonstrate force-activated mechanochemistry in hydrogels for molecular release for the first-time. Key to this advance is the use of a double network hydrogel of polyacrylamide and alginate that imbue the material with high toughness, thereby allowing considerably more deformation to enhance molecular release via the retro Diels–Alder reaction. Boydston and Larsen introduced the concept of flex-mediated release through a retro-Diels-Alder reaction from an oxanorbornadiene mechanophore-based polymer material.[31] Subsequently, there were several reports exploring this molecular release approach,[39] including cascading reactions[35] and activation in aqueous environments[40, 41] Inspired by these studies, we proposed that mechanophore-liked hydrogels may more readily undergo activation compared to dry polymers.

Bo and Zang have shown that the rate of mechanochemical activation for the furan/maleimide adduct depends on the polymer arms' relative proximity (proximal vs. distal) to the scissile bond, with proximal positioning demonstrating higher activation[42] We designed a Diels-Alder adduct mechanophore (Oxo-OBn) formed by alkyne/furan Diels-Alder cycloaddition to contain a pendent molecule proximal to the scissile bond (Fig. 1; Fig. S1-S3). We synthesized the Oxo-OBn mechanophore

molecule by first reacting bis(6-hydroxyhexyl)but-2-ynedioate and 2-((benzyloxy)methyl)furan Next, we performed Fischer esterification between acetylene dicarboxylate and 1,6-hexanediol. The benzyl furfuryl ether was formed through a reaction between furan-2-yl methanol and (chloromethyl)benzene followed by cycloaddition with the alkyne. Finally, the reaction with methacryloyl anhydride yielded the Oxo-OBn crosslinker. Nuclear magnetic resonance spectroscopy (NMR) confirmed the synthesized molecular structure at each step (Fig. S4-S6).

To incorporate the Oxo-OBn mechanophore into a hydrogel network, we substituted the mechanophore in place of bis-acrylamide as the crosslinking agent with DMSO as solvent and ammonium persulfate as radical initiator (Fig. 2A). After complete washout of DMSO monitored using FTIR (Fig. S7), we performed preliminary mechanical tests of as-prepared single network hydrogel samples. The hydrogels showed brittle failure under tension and compression with no evidence of mechanophore activation and molecule release (data not shown). To combat the low strength and toughness of the mechanophore-linked polyacrylamide gel network, we fabricated double network hydrogels consisting of two interpenetrating polymer networks, where a densely crosslinked brittle network is supported by a flexible network with reversible bonds.[43, 44] In response to stress, the densely crosslinked network will rupture locally, generating internal damage and dissipating energy, while the flexible polymer network remains well crosslinked and keeps the material intact. To test the double network hydrogel concept in our mechanophore-linked network, we incorporated ionically crosslinked alginate as a secondary network within the monomer solution prior to crosslinking to yield a mechanosensitive double-network hydrogel (Fig. 2A).

To characterize the hydrogel assembly, we performed Raman spectroscopy. The peaks from the polyacrylamide and Oxo-OBn spectra are summarized in Supporting Information, Table S1. The spectrum of Oxo-OBn linked polyacrylamide gel features peaks associated with benzene ring breathing (1,000 cm^{-1}) and norbornadiene CH wagging (677 cm^{-1}) (Fig. 2B, Table S2). Next, we acquired the spectra surface mapping at 677 cm^{-1} wavelengths of traditional bis-acrylamide and Oxo-OBn crosslinked polyacrylamide to show the mechanophore distribution, which confirms the presence of mechanophores throughout the hydrogel (Fig. 2C). Moreover, curve fitting of

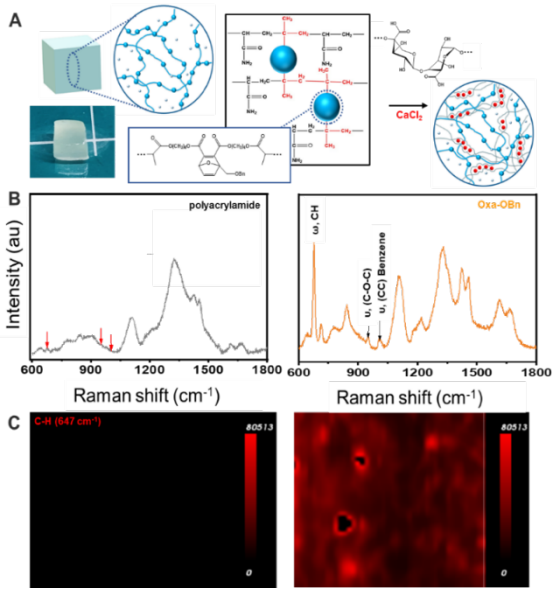

Fig. 2 A. Schematic with accompanying photograph of mechanophores integrated into double network hydrogel. B. Raman spectrum for the bis-acrylamide crosslinked polyacrylamide hydrogel (left) and the oxanorbornadiene crosslinked polyacrylamide hydrogel (right). C. Raman scan of the C-H wagging mode at 647 cm^{-1} for bis-acrylamide (left) and oxanorbornadiene (right) crosslined polyacrylamide.

the Raman spectrum across the 1400-800 cm^{-1} wavelength range reveals a peak at 1516 cm^{-1} for C=C stretching[45] corresponding to the double bonds in the oxanorbornadiene ring (Fig. S8)

After radical polymerisation of the Oxo-OBn and acrylamide, the samples were immersed in $CaCl_2$ solution to stabilize the alginate network and stored overnight. Swelling analysis indicates the as-prepared hydrogel swelled 1.4-1.5x after incubation (Figure S9). The sample was removed from the solution, excess water discarded and immediately subjected to compression testing. Compression tests were performed at room temperature to examine the double network hydrogel mechanical properties and mechanochemical reactivity. The original report of tough hydrogels based on polyacrylamide and alginate reported a hydrogel Young's modulus of 29 kPa.[46] Using a similar recipe, double network hydrogels were formed with mechanophore concentrations of 5 wt% and 10 wt%, where the di- methacrylate mechanophore serves as a replacement for bis-acrylamide. We increased the mechanophore concentration

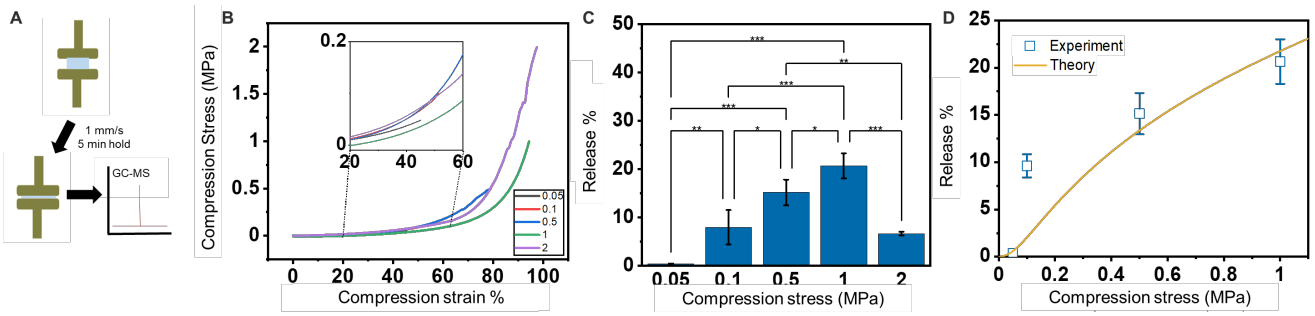

Fig. 3 A. Scheme for compression testing and eluent analysis. B. Engineering stress-engineering strain curves for the mechanophore crosslinked hydrogel (5 wt.%) with a 1 mm/minute compression, 5 min hold at 0.05, 0.1 , 0.5, 1, and 2 MPa. C. Percentage release from mechanophores under various compression stresses along with the results of the statistical tests (*P <= 0.05, **P <= 0.01, ***P <= 0.001 one-way ANOVA analysis). D. Release-strain relationship for observed molecule release vs theoretical prediction.

up to 30 wt %; however, those materials were exceptionally brittle under compression and were not further studied. The 5% mechanophore loaded double gel can reach a engineering strain of greater that 90% under compression without failing, and it has an elastic modulus of approximately 58 kPa (Fig. 3B and S10). Previous work exploring retro Diels- Alder release of mechanophores from polymers proposed holding times are necessary for the stress field to equilibrate and induce flex activation during compression.[31] The double network hydrogel samples were held under sustained stress for five minutes followed by rinsing with water and immersion in dichloromethane overnight to collect the released furfuryl ether molecules in solution (Fig. 3A). The concentration of small molecules in the eluent was subsequently measured via gas chromatography-mass spectrometry (GC-MS, Fig. S11) where a non-compressed sample was used as a control. Further details of sample preparation for compression testing can be found in the supplementary information. We tested gels under a broad range of compression stresses from 10 kPa to 2MPa (Fig. 3B). The materials behave elastically under stress <0.5 MPa. However, some plastic deformation occurred in samples exposed to stress ≥0.5 MPa and with repeated loading (Fig. S9B), which poses limitations on their use in high stress applications. Analysis of the eluent from compressed hydrogels indicates no molecule release at 10 kPa with evidence for marginal release at 50 kPa with an increase corresponding to applied force. We observe the highest activation of ~20% released molecules at 1 MPa compression. This in in sharp contrast to previous work, where flex-activation in dry polymer systems showed a maximum of 6-7% release at 35 MPa of force.[31] Above 1 MPa we observe failure of the specimens and network rupture, corresponding to a decrease in molecular release (Fig. 3B and C). A theoretical model for mechanochemically active elastomer and gels was then customized to this material in order to better understand this progression in small molecule release (details in SI).[47] The model shows a similar non-linear release behavior with stress as seen experimentally (Fig. 3D and S12).

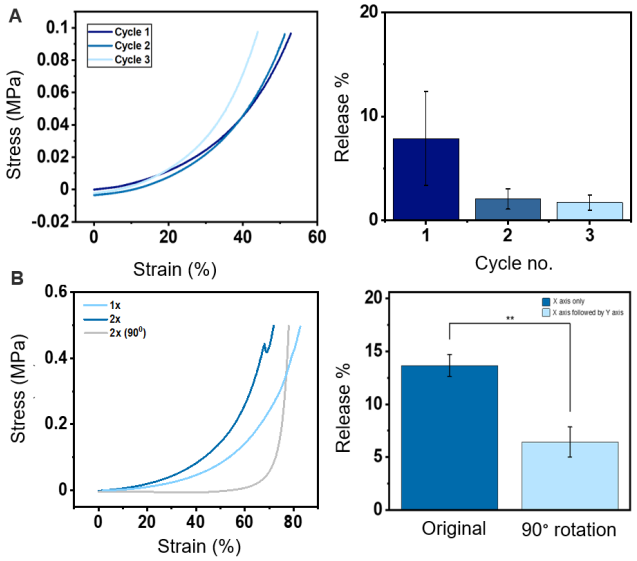

Fig. 4A. Stress-strain relationship for mechanophore crosslinked hydrogels (5 wt.%) with 1 mmmin-1 compression and 5 min hold for successive compressions. Percentage release from mechanophores from the same sample at successive compressions. B. Stress-strain relationship for mechanophore crosslinked hydrogels (5 wt.%) with 1 mm min^{-1} compression and 5 min hold after directional compression. Percentage activation of mechanophores on a sample (5 wt.%) after compression and after 90° rotation along with the results of the statistical tests (*P <= 0.05, **P <= 0.01, ***P <= 0.001 one-way ANOVA analysis).

Next, we asked whether the remaining mechanophores within the double network would be accessible through repeated cycles of loading. To test this, we compressed samples at 0.1 MPa with 1 mm min^{-1} compression rate followed by collection of eluent and analysis by GC-MS between each cycle. There was a diminishing amount of molecule release under successive compressions of the same sample (Fig. 4A). This was expected since the mechanophores that were initially well oriented for release at those stress levels were triggered on the first cycle. In this case, the release upon reloading is thought to be mostly due to a slight rearrangement in the network caused by prior to microdamage. Even after an additional seven cycles of compression (10x total) the quantity of released molecule is <20% total. To further demonstrate this orientation effect, we compressed samples as before, removed the stress, rotated the sample by 90-degs, and reapplied 0.1 MPa compression. As shown in Fig. 4B, the samples show substantially more release after rotation than after repeat cycling in the same direction. The reduction in release of the rotated samples compared to that of initial loading is similar to that predicted by our double network mechanochemical release model (Fig. S13), and this decrease primarily originates from some release occurring along polymer chains transverse to the loading direction under the first compression.

In conclusion, we demonstrate how integrating flex-activated mechanophores into double network hydrogels facilitates molecular release at forces several orders of magnitude lower than previously reported studies in dry polymers. We propose this enhanced mechanochemical response is due to a combination of the aqueous environment and the interpenetrating tough network allowing high degrees of deformation while the samples remain intact. Hydrogels are ubiquitous in society, serving important roles in applications spanning biomedical materials, devices, and biotechnology. Therefore, this work paves the way to mechanosensitive molecule releasing materials such as force-sensitive drug releasing scaffolds, contact lenses, bandages, orthopedic coatings, or device components.

We acknowledge the facilities provided by the Mark Wainwright Analytical Centre, University of New South wales. Financial support was provided by the Australian Research Council grants FT180100417 and DP210103654 and by the National Science Foundation under Grant No. CAREER-1653059. The authors declare no conflict of interest.

1. J. Li, C. Nagamani and J. S. Moore, *Acc. Chem. Res.*, 2015, **48**, 2181-2190.
2. M. Abi Ghanem, A. Basu, R. Behrou, N. Boechler, A. J. Boydston, S. L. Craig, Y. Lin, B. E. Lynde, A. Nelson and H. Shen, *Nat. Rev. Mater.*, 2020, 1-15.
3. H. Staudinger and H. Bondy, *Rubber Chem. Technol.*, 1930, **3**, 519-521.
4. A. L. Black, J. M. Lenhardt and S. L. Craig, *J. Mater.Chem.*, 2011, **21**, 1655-1663.

5. N. R. Sottos, *Nature chemistry*, 2014, **6**, 381.
6. P. A. May and J. S. Moore, *Chem. Soc. Rev.*, 2013, **42**, 7497-7506.
7. Y. Chen, G. Mellot, D. van Luijk, C. Creton and R. P. Sijbesma, *Chem. Soc. Rev.*, 2021.
8. C. K. Lee, B. A. Beiermann, M. N. Silberstein, J. Wang, J. S. Moore, N. R. Sottos and P. V. Braun, *Macromolecules*, 2013, **46**, 3746-3752.
9. Y. Chen, A. Spiering, S. Karthikeyan, G. W. Peters, E. Meijer and R. P. Sijbesma, *Nat. Chem.*, 2012, **4**, 559.
10. M. J. Robb and J. S. Moore, *J. Am. Chem. Soc.*, 2015, **137**, 10946-10949.
11. M. J. Kryger, M. T. Ong, S. A. Odom, N. R. Sottos, S. R. White, T. J. Martinez and J. S. Moore, *J. Am. Chem. Soc.*, 2010, **132**, 4558-4559.
12. M. Karman, E. Verde-Sesto, C. Weder and Y. C. Simon, *ACS Macro Lett.*, 2018, **7**, 1099-1104.
13. Y. Sagara, M. Karman, E. Verde-Sesto, K. Matsuo, Y. Kim, N. Tamaoki and C. Weder, *J. Am. Chem. Soc.*, 2018, **140**, 1584-1587.
14. T. Xia, W. Liu and L. Yang, *J. Biomed. Mater.Res. A*, 2017, **105**, 1799-1812.
15. B. H. Bowser and S. L. Craig, *Polym. Chem.*, 2018, **9**, 3583-3593.
16. R. W. Barber, M. E. McFadden, X. Hu and M. J. Robb, *Synlett*, 2019, **30**, 1725-1732.
17. N. Deneke, M. L. Rencheck and C. S. Davis, *Soft Matter*, 2020, **16**, 6230-6252.
18. J. Wang, T. B. Kouznetsova, Z. S. Kean, L. Fan, B. D. Mar, T. J. Martínez and S. L. Craig, *J. Am. Chem. Soc.*, 2014, **136**, 15162-15165.
19. M. A. Ghanem, A. Basu, R. Behrou, N. Boechler, A. J. Boydston, S. L. Craig, Y. Lin, B. E. Lynde, A. Nelson, H. Shen and D. W. Storti, *Nat. Rev. Mater.*, 2020, **6**, 84-98.
20. R. C. Rohde, A. Basu, L. B. Okello, M. H. Barbee, Y. Zhang, O. D. Velev, A. Nelson and S. L. Craig, *Polym. Chem.*, 2019, **10**, 5985-5991.
21. D. A. Davis, A. Hamilton, J. Yang, L. D. Cremar, D. Van Gough, S. L. Potisek, M. T. Ong, P. V. Braun, T. J. Martinez, S. R. White, J. S. Moore and N. R. Sottos, *Nature*, 2009, **459**, 68-72.
22. C. Calvino, A. Guha, C. Weder and S. Schrettl, *Adv. Mater.*, 2018, **30**, e1704603.
23. M. E. Grady, B. A. Beiermann, J. S. Moore and N. R. Sottos, *ACS Appl. Mater. Interfaces*, 2014, **6**, 5350-5355.
24. G. I. Peterson, M. B. Larsen, M. A. Ganter, D. W. Storti and A. J. Boydston, *ACS Appl. Mater. Interfaces*, 2015, **7**, 577-583.
25. A. Piermattei, S. Karthikeyan and R. P. Sijbesma, *Nature chemistry*, 2009, **1**, 133-137.
26. C. E. Diesendruck, B. D. Steinberg, N. Sugai, M. N. Silberstein, N. R. Sottos, S. R. White, P. V. Braun and J. S. Moore, *J. Am. Chem. Soc.*, 2012, **134**, 12446-12449.
27. R. Gunckel, B. Koo, Y. Xu, B. Pauley, A. Hall, A. Chattopadhyay and L. L. Dai, *ACS Appl. Polym. Mater.*, 2020, **2**, 3916-3928.
28. G. R. Gossweiler, G. B. Hewage, G. Soriano, Q. Wang, G. W. Welshofer, X. Zhao and S. L. Craig, *ACS Macro Lett.*, 2014, **3**, 216-219.
29. M. J. Robb and J. S. Moore, *J. Am. Chem. Soc.*, 2015, **137**, 10946-10949.
30. C. E. Diesendruck, G. I. Peterson, H. J. Kulik, J. A. Kaitz, B. D. Mar, P. A. May, S. R. White, T. J. Martínez, A. J. Boydston and J. S. Moore, *Nat. Chem.*, 2014, **6**, 623-628.
31. M. B. Larsen and A. J. Boydston, *J. Am. Chem. Soc.*, 2014, **136**, 1276-1279.
32. X. Hu, T. Zeng, C. C. Husic and M. J. Robb, *J. Am. Chem. Soc.c*, 2019, **141**, 15018-15023.
33. N. R. Sottos, *Nat. Chem.*, 2014, **6**, 381-383.
34. P. Lavalle, F. Boulmedais, P. Schaaf and L. Jierry, *Langmuir*, 2016, **32**, 7265-7276.
35. L. Wang, W. Zhou, Q. Tang, H. Yang, Q. Zhou and X. Zhang, *Polymers*, 2018, **10**, 994.
36. W. C. Ballance, Y. Seo, K. Baek, M. Chalifoux, D. Kim and H. Kong, *J. Control Release*, 2018, **275**, 1-11.
37. J. Chen, Q. Peng, X. Peng, L. Han, X. Wang, J. Wang and H. Zeng, *ACS Appl. Polym. Mater.*, 2020, **2**, 1092-1107.
38. T. Matsuda, R. Kawakami, R. Namba, T. Nakajima and J. P. Gong, *Science*, 2019, **363**, 504-508.
39. L. J. Mier, G. Adam, S. Kumar and T. Stauch, *Chem.Phys.Chem.*, 2020, **21**, 2402.
40. J. W. Wijnen and J. B. Engberts, *J. Org. Chem.*, 1997, **62**, 2039-2044.
41. G. K. van Der Wel, J. W. Wijnen and J. B. Engberts, *J. Org. Chem.*, 1996, **61**, 9001-9005.
42. R. Stevenson and G. De Bo, *J. Am. Chem. Soc.*, 2017, **139**, 16768-16771.
43. X. Su and B. Chen, *Carbohydr. Polym.*, 2018, **197**, 497-507.
44. Y. Zhuang, F. Yu, H. Chen, J. Zheng, J. Ma and J. Chen, *J. Mater. Chem. A*, 2016, **4**, 10885-10892.
45. V. Novikov, V. Kuzmin, S. Kuznetsov, M. Darvin, J. Lademann, E. Sagitova, L. Y. Ustynyuk, K. Prokhorov and G. Y. Nikolaeva, *Spectrochim. Acta A Mol. Biomol. Spectrosc.*, 2021, **255**, 119668.
46. J.-Y. Sun, X. Zhao, W. R. Illeperuma, O. Chaudhuri, K. H. Oh, D. J. Mooney, J. J. Vlassak and Z. Suo, *Nature*, 2012, **489**, 133-136.
47. M. R. Buche and M. N. Silberstein, *arXiv preprint arXiv:2104.08866*, 2021.

Supplemental Information

Force-mediated molecule release from double network hydrogels

Pavithra B Jayathilaka, [a] Thomas G Molley, [b] Yuwan Huang,[c] M. Shariful Islam, [b] Michael Robert Buche, [d] Meredith Silberstein, [d] Jamie J. Kruzic, [c] Kristopher A. Kilian,[a,b*]

[a] School of Chemistry, University of New South Wales (UNSW Sydney), Sydney NSW 2052, Australia
[b] School of Materials Science, University of New South Wales (UNSW Sydney), Sydney NSW 2052, Australia
[c] Sibley School of Mechanical and Aerospace Engineering, Cornell University, Ithaca, NY, USA

Materials

All commercially available materials were obtained from Sigma-Aldrich and were used as they were received without further purification unless otherwise specified. $CaCl_2$, Acetylene dicarboxylate, toluene, Diethyl ether (Et_2O), $NaHCO_3$, NaCl, $MgSO_4$, Celite, Ethyl acetate, hexanes, ethanol, and DMSO were purchased from CAS Scientific's ChemSupply. Silica gel was purchased from Silicycle Inc. All chemicals were reagent grade or better.

Instrumentation and Analysis

NMR characterization

Synthesized samples were dissolved in $CDCl_3$ at a final concentration of 10 mg/ml and transferred to an NMR sample tube. ^{1}H NMR spectra were recorded on Bruker BioSpin 400.13 MHz spectrometer at 293 K with 8 scans and a delay of 5 s. Chemical shifts were reported in delta (δ) units and expressed in parts per million (ppm) downfield from tetramethylsilane (TMS) using $CDCl_3$, 1H: 0.0 ppm as an internal standard. ^{1}H NMR data was first phased, and baseline corrected (Bernstein polynomial fit, order 3) using MNOVa software (MestRelab Research S.L version: 14.0.0-23239).

FTIR characterization

Fourier Transform Infrared (FTIR) spectrometer with attenuated total reflectance (ATR) was used to characterize gel samples, and spectra were recorded on Spectrum software. Hydrogels and organic samples (opaque oils, solids, and powders ranging from 22 μm to 2.5 μm) were analysed from 450-4000 cm^{-1} wavelength range.

Raman spectroscopy

Gels were dried at room temperature for overnight to remove the water before Raman studies. All measurements were carried out at room temperature. Raman spectra were collected by Renishaw (inVia 2) Raman spectrometer coupled to a microscope (Leica.), and spectra were recorded on Wire 5.3 software. The microscope focused a diode laser (785 nm, 9.6 mW, with1200 l / mm grating) onto the sample (~0.8 µm spot size) on exciting through a 5x magnification lens (Leica) and collected the light scattered off the sample surface. The scattered light was directed through the Raman spectrometer to obtain spectral data. Spectra were recorded from 600 cm^{-1} to 1800 cm^{-1}.

Experimental Procedures:

Synthesis

Step 1:

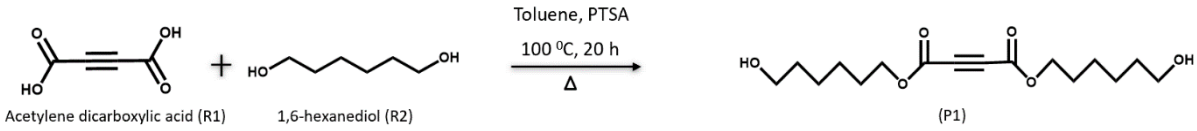

Figure S1: Mechanophore synthesis reaction step 1

Synthesis protocols are based on the literature which were modified during the experiments.[63] Esterification reaction was performed with mixing acetylene dicarboxylate (5.0 g, 43.8 mmol), 1,6-hexanediol (52 g, 438 mmol) in 70 ml of toluene. The catalyst, p-toluenesulfonic acid monohydrate (PTSA) (833 mg, 4.38 mmol), was added to the mixture. The reaction proceeded for 20 h at 100 °C. The generated water during the reaction was collected using a Dean-Stark trap, which was fitted to the reflux condenser. After 20 h, around ca.1.2 ml of water was collected, and the setup was allowed to reach room temperature. The solution was diluted with Et_2O (50 mL) and cooled at -10 °C for 1 hour. Then the solution was decanted, and the precipitate was washed with an excess of Et_2O. The combined organic solution was washed with saturated $NaHCO_3$ solution (2 × 50 mL), water (4 × 50 mL), and brine (1 × 50 mL), respectively. The resultant organic layer was dried with Mg_2SO_4, followed by filtering through a Celite pad. The product was concentrated under a vacuum to evaporate solvents. The resultant product was a pale-yellow oil with a yield of 46%. 1H NMR (400 MHz, $CDCl_3$) δ 4.20 (t, 4H), 3.61 (t, 4H), 1.70 – 1.60 (m, 4H), 1.55(m, 4H), 1.40 – 1.30(m, 8H).

Step 2:

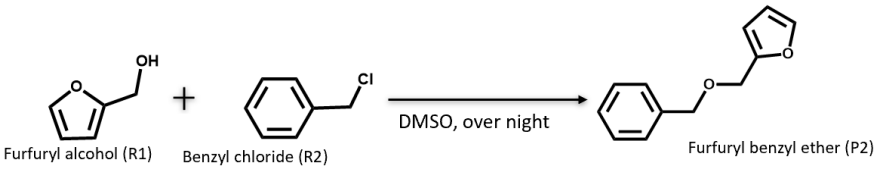

Figure S2: Mechanophore synthesis reaction step 2

Furfuryl alcohol was stirred in DMSO at room temperature overnight. After 1 h, benzyl chloride was added into the reaction mixture. The reaction was monitored via thin-layer chromatography (TLC). The crude product was purified with a silica column, and the yield was pale yellow liquid (98%).[64] 1H NMR (400 MHz, CDCl3) δ = 7.40–7.06 (m, 6H,), 6.26 (d, J = 4.0 Hz), 4.47 (s, 2H), 4.41 (s, 2H,)

Step 3:

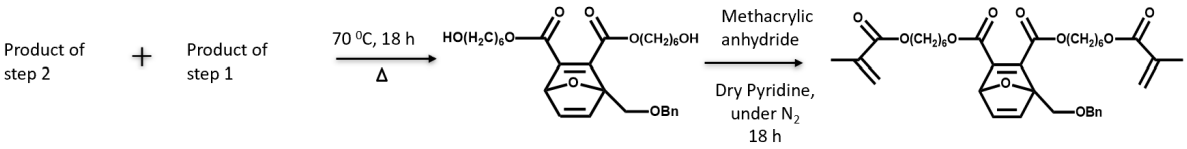

Figure S3: Mechanophore synthesis reaction step 3

Product of step 1 reaction (P1) (3.5 g, 11.1 mmol) and the product from step 2 (P2) of 2.31 g, 12.2 mmol, were reacted at 70 °C for 20 hours in a sealed vial. The reaction was monitored via ^{1}H NMR spectroscopy. When the reaction was completed, the mixture was allowed to come to room temperature. Then the excess unreacted starting materials were removed by triturating with hexane ((3 × 15 mL). Excess solvent was removed under vacuum, and the intermediate diol yield was dark orange oil (70%)

The intermediate diol was reacted with (298 mg, 0.59 mmol) methacrylic anhydride (660 µL, 4.4 mmol) in dry pyridine under an N_2 environment for 18 h. The reaction was monitored with TLC (85% EtOAc/hexanes). The mixture was diluted with Et2O (10 mL) and successively washed with water (2 × 10 mL) and 10 wt% $CuSO_4$ solutions (3 × 10 mL) followed by saturated $NaHCO_3$ solution (2 × 10 mL). The resultant organic layer was dried with Mg_2SO_4 and vacuumed to get the crude product. The crude product was purified with flash column chromatography (20% EtOAc/hexanes) (R_f = 0.85). The yield was pale yellow oil (9.5%). 1H NMR (400 MHz,

$CDCl_3$) δ 7.40 – 7.29 (m, 5H), 7.20 (s, 1H), 6.99 (d, *J* = 5.2 Hz, 1H), 6.09 (s, 2H), 5.70 (s, 1H), 5.55 (s, 2H), , 462 (s,2H), 4.55 (s,2H), 4.23 – 4.07 (m, 8H), 1.94 (s, 6H), 1.70 – 1.62 (m, 8H), 1.45 – 1.35 (m, 8H).

Step 1 product (P1) –

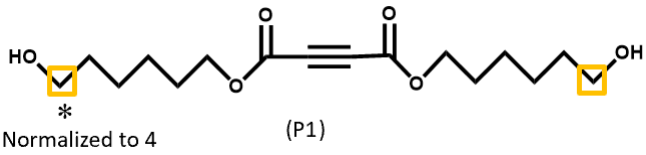

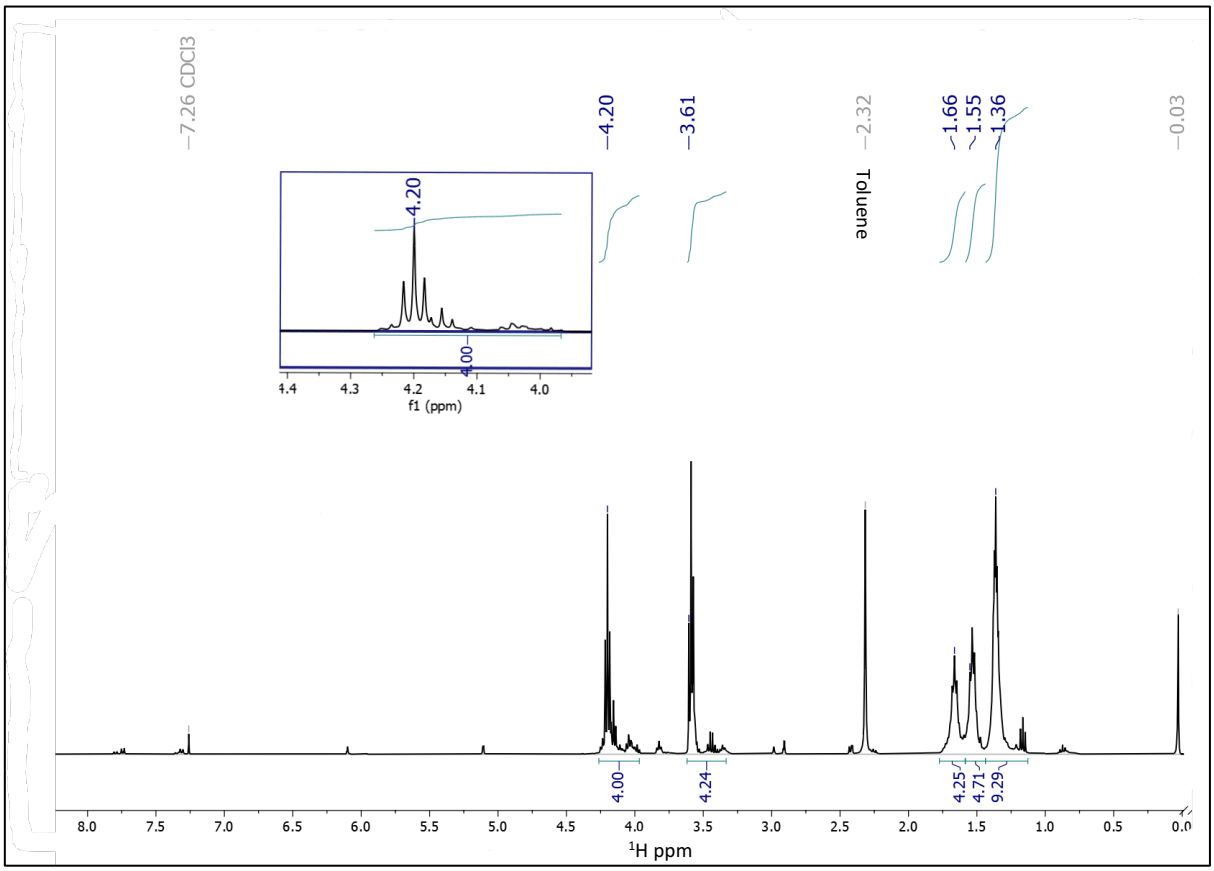

Figure S4: ^{1}H NMR spectrum of P1. Inset: magnified 4.4– 4.0 ppm region

Step 2 product (P2) :

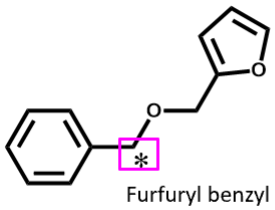

Furfuryl benzyl ether (P2)

Normalized to 2

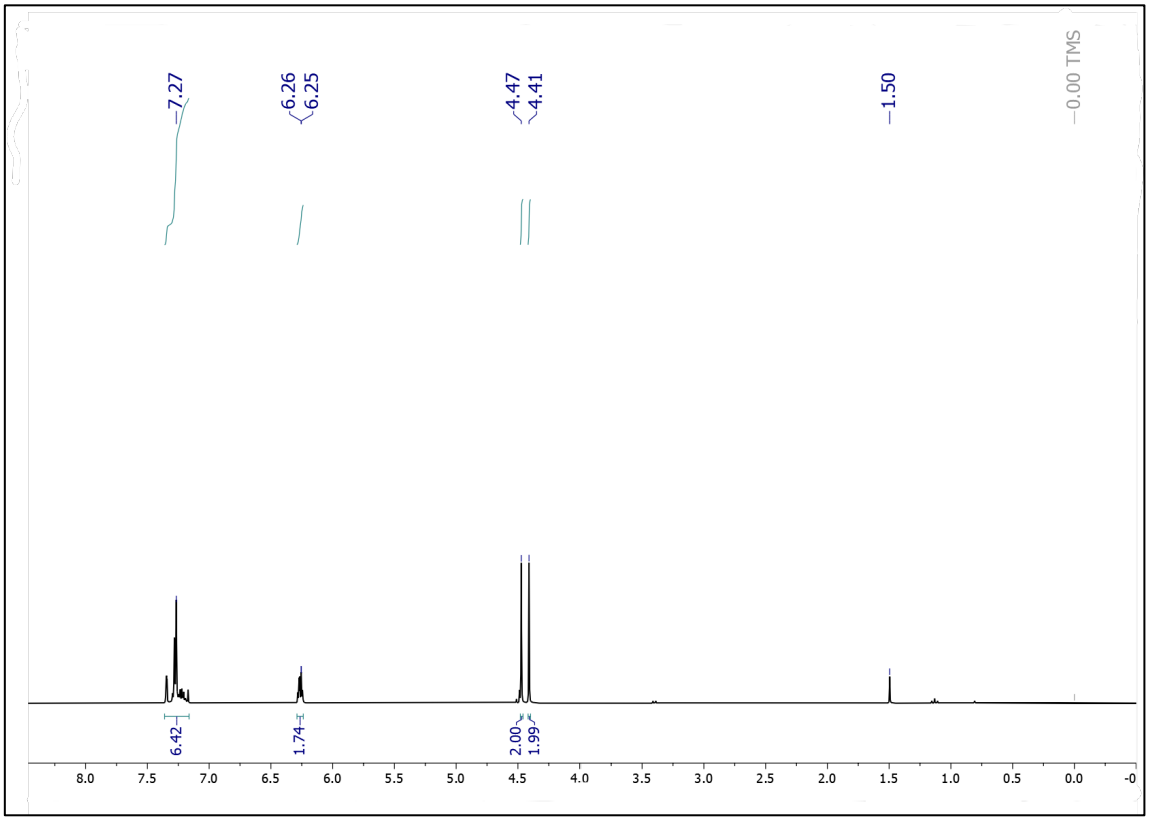

Figure S5: ^{1}H NMR spectrum of P2

Step 3 mechanophore –

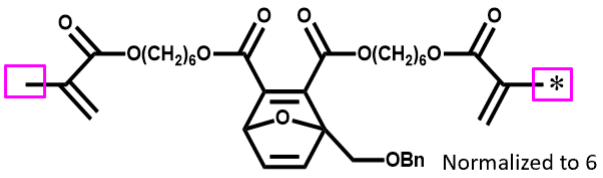

Figure S6: ^{1}H NMR spectrum of mechanophore

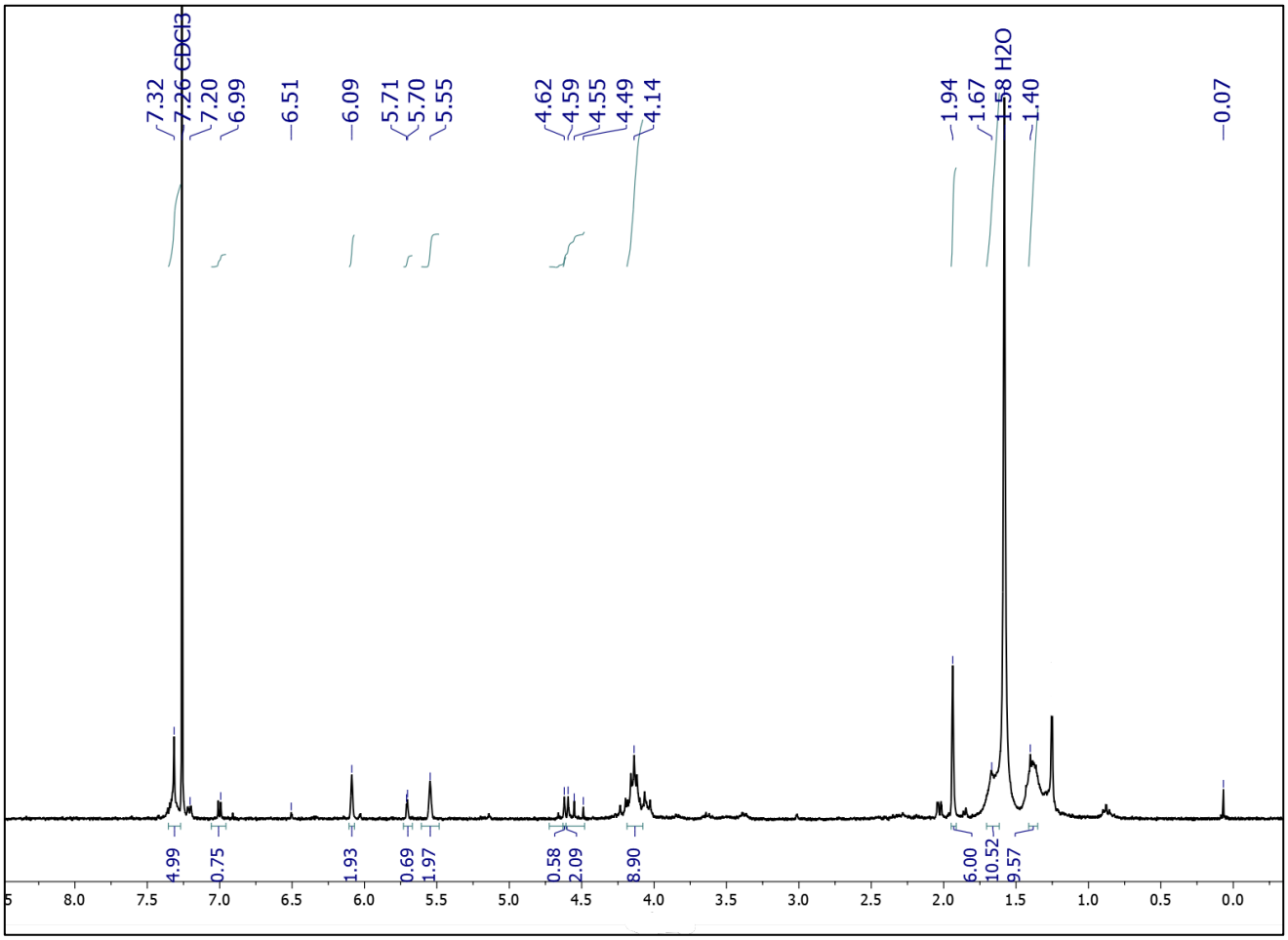

Preparation of double network hydrogels

5 wt% oxanorbornadiene mechanophore in DMSO was dissolved in 95 wt% acrylamide containing 1.45 wt% alginate with a final volume of 1 mL. Ammonium persulphate (5.0 µL) as a photo-initiator and N,N,N',N'-tetramethylethylenediamine (TEMED) (0.5 µL) as the crosslinking accelerator were added to the mixture. The solution was poured into a glass mold for the covalent network to polymerize. After 45 min of gelation time, the hydrogel was washed with water to remove DMSO with DMSO removal monitored with FTIR. After complete removal of DMSO the sample was immersed in 3 wt% $CaCl_2$ solution overnight and stored until use.

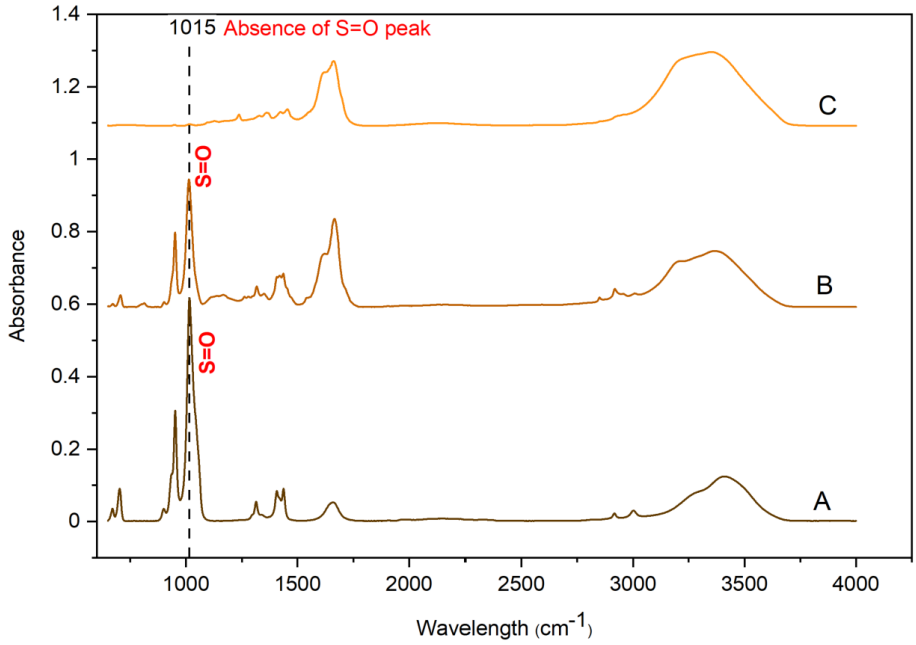

Figure S7: Evaluation of DMSO removal by FTIR. a) FTIR spectrum of DMSO, which shows characteristic S=O bond peak at 1015 cm ^{1}. b) FTIR spectrum of the hydrogel before removing DMSO. c) FTIR spectrum of the hydrogel before removing DMSO, which confirms the removal of DMSO by the absence of S=O peak at 1015 cm^{-1}.

Mechanical tests

Specimens were removed from the $CaCl_2$ storage solution, excess fluid removed with shaking and wicking with a Kim wipe, and immediately subjected to compression in a humid environment. The compression tests were performed by a universal testing instrument (ElectroPuls E1000, Instron) with a 250 N load cell (Instron). The test speed was 1 mm/min, and the load was held on the sample for 5 min. Engineering stress-strain curves were presented after tests. The strain and stress were calculated using the two equation $\varepsilon_e = \frac{\Delta h}{h_o}$ and $\sigma_e = \frac{F}{A_0}$, where h_0 and A_0 are the original height and cross-sectional area of the uncompressed sample, Δh is the change in height, *F*

is the applied force. The compressive modulus was defined as the ratio of stress to strain in the initial compression region and determined using the average slope of fitting line within 5-10% strain range.

Mechanical test was performed on cubic samples following table shows each dimension.

TABLE 1 Sample dimensions

Compression stress	*Dimensions (mm)*
0.01 MPa	*6.20 × 5.60 × 5.40*
0.05 MPa	*5.80 × 5.60 × 5.90*
0.10 MPa	*5.70 × 5.00 × 4.90*
0.05 MPa	*4.80 × 5.00 × 4.50*
1.00 MPa	*5.00 × 4.50 × 5.40*
2.00 MPa	*4.50 × 4.20 × 5.20*

GC-MS analysis

Molecule release under compression was monitored with gas chromatography-mass spectrometry (GC-MS). GC analysis were carried out using a Shimadzu GCMS QP2010Plus with diphenyl/methyl column (30m × 0.32mm × 0.25 μm film thickness on GC system with a flame ionization detector (FID)

Data analysis

All Raman, FTIR, and GC-MS acquired data were analyzed by Origin2020b software. Origin2020b software was used for the statistical analysis to show differences between groups (One-way ANOVA). Significant difference is indicated when $P < 0.05$.

The percentage of molecule was calculated as

$$Release\ \% = \frac{amount\ of\ molecule\ release\ (g) \times 100}{amount\ of\ molecules\ loaded\ on\ gel(g)}$$

TABLE 2 Assignment of Raman bands

Reported (cm^{-1})[65-67]	Observed in this work		Assignment
	PAAm	Oxo	
641	641	644	τ, CH_2
667 [66]		677	Norbornadiene ω, CH
780	779	775	ω, CH
844	842	844	Γ, CH2
800-970 [68]		951	υ, (C-O-C)
1000 [68]		1005	υ, (CC) aromatic ring
1113	1107	1111	υ, (C-C)
1209	1212	1220	ω, NH_2
1326	1324	1328	δ, CH
1430	1429	1422	υ, C-N
1457	1452	1456	δ, CH_2
1516		1516	Norbornadiene C=C
1607	1608	1616	δ, NH_2
1665	1669	1664	υ, C=O in amide

v_a and v_s - asymmetric and symmetric stretching, δ - bending, ω - wagging, Γ - twisting, τ - torsion

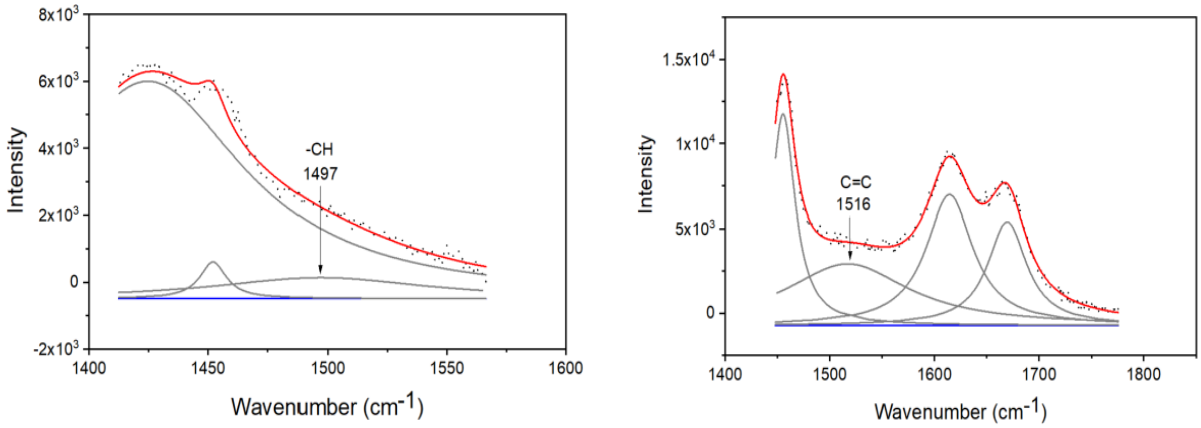

Figure S8: Curve fitting Raman spectra with deconvolution into the Lorentz components after baseline subtraction a) Acrylamide gel (control) b) mechanophore-linked hydrogel, which shows the presence of C=C bond of oxanorbornadiene mechanophore

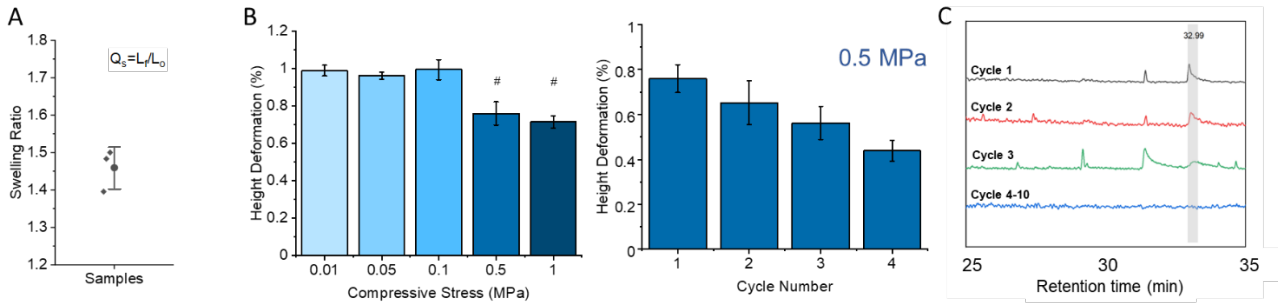

Figure S9. (a) Swelling analysis for mechanophore crosslinked double network hydrogels. (b) change in specimen geometry after compression at different forces (left) and during cyclic loading at 0.5 MPa (right). (c) GC elution analysis of samples compressed in the same direction up to ten times. #signifies p<0.005 compared to 0.01, 0.05 and 0.1 MPa compression.

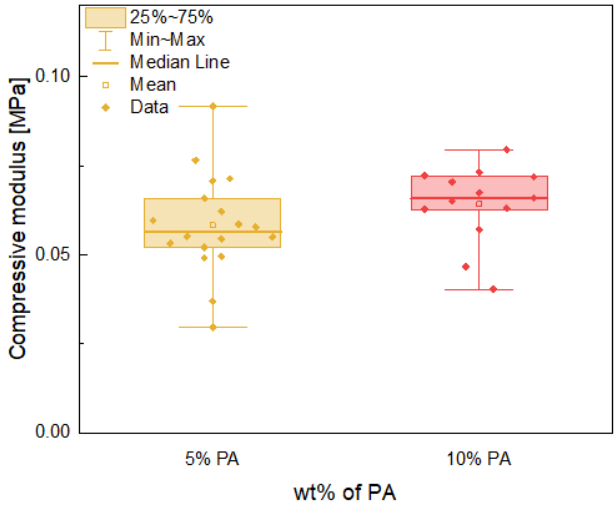

Figure S10: Box and whisker plots of the compressive modulus of 5% and 10% mechanophore containing samples based on 18 repeat experiments for the 5% case and 13 repeat experiments for the 10% case.

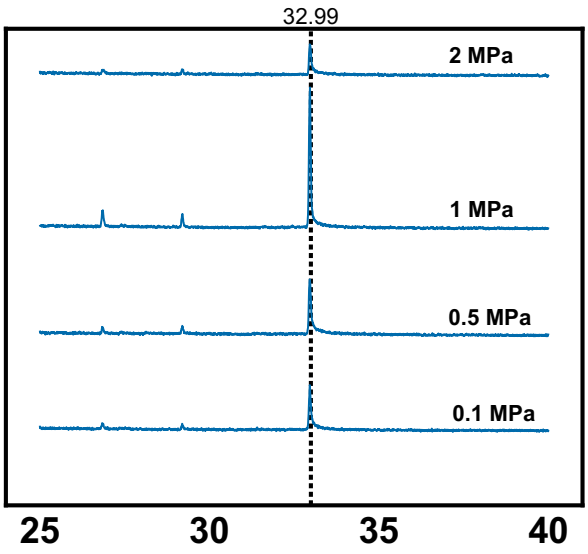

Figure S11: GC-MS trace showing elution of the Oxo-OBn molecular release.

Theoretical modelling of molecule release

The model for small molecule release in the double network hydrogel was adapted from [62] to include an irreversible reaction (molecule release) that does not result in fracture of the polymer chains, in addition to a later irreversible scission of the chains. In brief, this model starts from the statistical mechanical description of a single polymer chain and predicts the stress response and mechanochemical response of the polymer network when subjected to mechanical deformation. The parameters in this model are the number of links in a single chain segment, N_b; the volumetric swelling ratio, J; the total number density of chains, n; the nondimensional link stiffness, κ; the nondimensional end-to-end length of the chain that triggers the release, $\gamma_{release}$; and the nondimensional end-to-end length that results in scission of the chain, $\gamma_{scission}$. The values for these parameters are given in Table 2. The first three parameters were directly determined by the polymer chemistry: N_b was determined by the average number of monomers between crosslinks; J was estimated from the water content compared to the dry polymer content; and nkT was determined such that the model matched the median elastic modulus from the experiments of 56 kPa. κ and $\gamma_{scission}$ were calibrated to the mechanical response of the material, while $\gamma_{release}$ was then calibrated to the corresponding release percentage. [62] The model is stiffer than the experimental data at large strain primarily because we neglect the increase in contour length that results from the small molecule release.

TABLE 2. Parameters for double network hydrogel model

Parameter	Value
N_b	85
J	10
nkT	36.56 kPa
κ	2000
$\gamma_{release}$	0.575
$\gamma_{scission}$	1

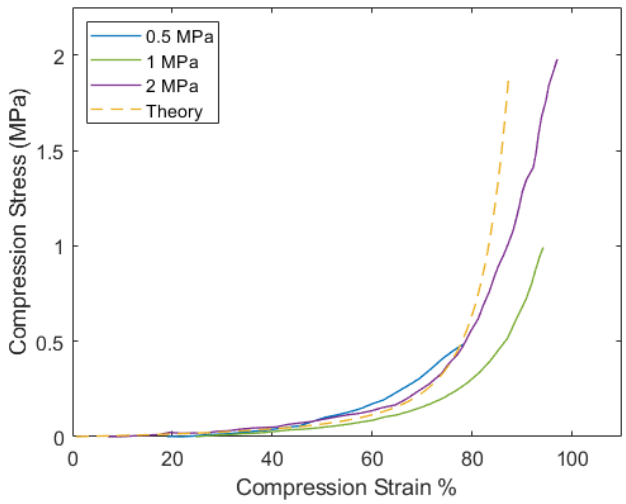

Figure S12: Engineering stress-strain plots of experimental data for the 5% gel compression alongside the theoretical model

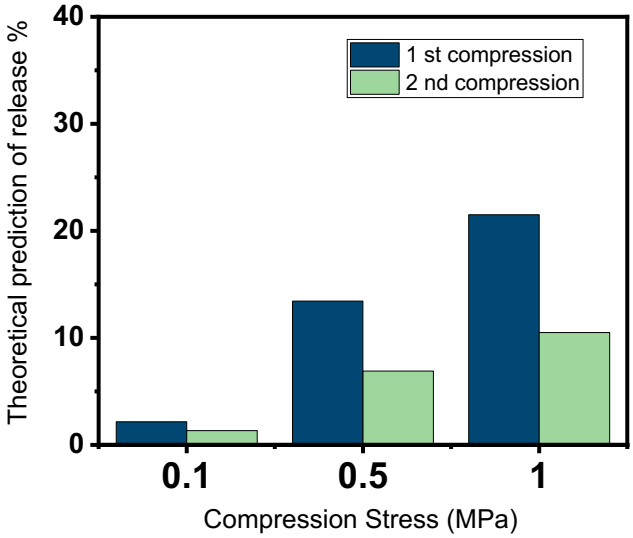

Figure S13. Theoretical molecule release predicted after the first compression and the second compression with 90° rotation.

References

1. Larsen, M. B.; Boydston, A. J., Investigations in fundamental and applied polymer mechanochemistry. *Macromolecular Chemistry and Physics* **2016,** *217* (3), 354-364.
2. Costa, A. M.; Mano, J. F., Extremely strong and tough hydrogels as prospective candidates for tissue repair–A review. *European Polymer Journal* **2015,** *72*, 344-364.
3. Li, J.; Nagamani, C.; Moore, J. S., Polymer mechanochemistry: from destructive to productive. *Accounts of chemical research* **2015,** *48* (8), 2181-2190.
4. Facchi, D. P.; Cazetta, A. L.; Canesin, E. A.; Almeida, V. C.; Bonafé, E. G.; Kipper, M. J.; Martins, A. F., New magnetic chitosan/alginate/Fe3O4@ SiO2 hydrogel composites applied for removal of Pb (II) ions from aqueous systems. *Chemical Engineering Journal* **2018,** *337*, 595-608.
5. Abi Ghanem, M.; Basu, A.; Behrou, R.; Boechler, N.; Boydston, A. J.; Craig, S. L.; Lin, Y.; Lynde, B. E.; Nelson, A.; Shen, H., The role of polymer mechanochemistry in responsive materials and additive manufacturing. *Nature Reviews Materials* **2020**, 1-15.
6. Staudinger, H.; Bondy, H., Isoprene and rubber. XIX. The molecular size of rubber and balata. *Rubber Chemistry and Technology* **1930,** *3* (3), 519-521.
7. Black, A. L.; Lenhardt, J. M.; Craig, S. L., From molecular mechanochemistry to stress-responsive materials. *Journal of Materials Chemistry* **2011,** *21* (6), 1655-1663.
8. Sottos, N. R., Polymer mechanochemistry: Flex, release and repeat. *Nature chemistry* **2014,** *6* (5), 381.
9. Brantley, J. N.; Wiggins, K. M.; Bielawski, C. W., Polymer mechanochemistry: the design and study of mechanophores. *Polymer international* **2013,** *62* (1), 2-12.
10. May, P. A.; Moore, J. S., Polymer mechanochemistry: techniques to generate molecular force via elongational flows. *Chemical Society Reviews* **2013,** *42* (18), 7497-7506.
11. Beiermann, B. A.; Kramer, S. L.; Moore, J. S.; White, S. R.; Sottos, N. R., Role of mechanophore orientation in mechanochemical reactions. *Acs Macro Letters* **2012,** *1* (1), 163-166.
12. Beiermann, B. A.; Davis, D. A.; Kramer, S. L.; Moore, J. S.; Sottos, N. R.; White, S. R., Environmental effects on mechanochemical activation of spiropyran in linear PMMA. *Journal of Materials Chemistry* **2011,** *21* (23), 8443-8447.
13. Beiermann, B. A.; Kramer, S. L.; May, P. A.; Moore, J. S.; White, S. R.; Sottos, N. R., The effect of polymer chain alignment and relaxation on force-induced chemical reactions in an elastomer. *Advanced Functional Materials* **2014,** *24* (11), 1529-1537.

14. Chen, Y.; Mellot, G.; van Luijk, D.; Creton, C.; Sijbesma, R. P., Mechanochemical tools for polymer materials. *Chemical Society Reviews* **2021**.
15. Davis, D. A.; Hamilton, A.; Yang, J.; Cremar, L. D.; Van Gough, D.; Potisek, S. L.; Ong, M. T.; Braun, P. V.; Martínez, T. J.; White, S. R., Force-induced activation of covalent bonds in mechanoresponsive polymeric materials. *Nature* **2009,** *459* (7243), 68-72.
16. Degen, C. M.; May, P. A.; Moore, J. S.; White, S. R.; Sottos, N. R., Time-dependent mechanochemical response of SP-cross-linked PMMA. *Macromolecules* **2013,** *46* (22), 8917-8921.
17. Lee, C. K.; Beiermann, B. A.; Silberstein, M. N.; Wang, J.; Moore, J. S.; Sottos, N. R.; Braun, P. V., Exploiting force sensitive spiropyrans as molecular level probes. *Macromolecules* **2013,** *46* (10), 3746-3752.
18. Li, M.; Zhang, Q.; Zhou, Y.-N.; Zhu, S., Let spiropyran help polymers feel force! *Progress in Polymer Science* **2018,** *79*, 26-39.
19. Chen, Y.; Spiering, A.; Karthikeyan, S.; Peters, G. W.; Meijer, E.; Sijbesma, R. P., Mechanically induced chemiluminescence from polymers incorporating a 1, 2-dioxetane unit in the main chain. *Nature chemistry* **2012,** *4* (7), 559.
20. Robb, M. J.; Moore, J. S., A retro-staudinger cycloaddition: Mechanochemical cycloelimination of a β-lactam mechanophore. *Journal of the American Chemical Society* **2015,** *137* (34), 10946-10949.
21. Kryger, M. J.; Ong, M. T.; Odom, S. A.; Sottos, N. R.; White, S. R.; Martinez, T. J.; Moore, J. S., Masked cyanoacrylates unveiled by mechanical force. *Journal of the American Chemical Society* **2010,** *132* (13), 4558-4559.
22. Karman, M.; Verde-Sesto, E.; Weder, C.; Simon, Y. C., Mechanochemical Fluorescence Switching in Polymers Containing Dithiomaleimide Moieties. *ACS Macro Letters* **2018,** *7* (9), 1099-1104.
23. Sagara, Y.; Karman, M.; Verde-Sesto, E.; Matsuo, K.; Kim, Y.; Tamaoki, N.; Weder, C., Rotaxanes as mechanochromic fluorescent force transducers in polymers. *Journal of the American Chemical Society* **2018,** *140* (5), 1584-1587.
24. Black, A. L.; Orlicki, J. A.; Craig, S. L., Mechanochemically triggered bond formation in solid-state polymers. *Journal of Materials Chemistry* **2011,** *21* (23), 8460-8465.
25. Diesendruck, C. E.; Steinberg, B. D.; Sugai, N.; Silberstein, M. N.; Sottos, N. R.; White, S. R.; Braun, P. V.; Moore, J. S., Proton-coupled mechanochemical transduction: a mechanogenerated acid. *J Am Chem Soc* **2012,** *134* (30), 12446-9.
26. Xia, T.; Liu, W.; Yang, L., A review of gradient stiffness hydrogels used in tissue engineering and regenerative medicine. *Journal of Biomedical Materials Research Part A* **2017,** *105* (6), 1799-1812.
27. Bowser, B. H.; Craig, S. L., Empowering mechanochemistry with multi-mechanophore polymer architectures. *Polymer Chemistry* **2018,** *9* (26), 3583-3593.
28. Barber, R. W.; McFadden, M. E.; Hu, X.; Robb, M. J., Mechanochemically Gated Photoswitching: Expanding the Scope of Polymer Mechanochromism. *Synlett* **2019,** *30* (15), 1725-1732.
29. Deneke, N.; Rencheck, M. L.; Davis, C. S., An engineer's introduction to mechanophores. *Soft Matter* **2020,** *16* (27), 6230-6252.
30. Wang, J.; Kouznetsova, T. B.; Kean, Z. S.; Fan, L.; Mar, B. D.; Martínez, T. J.; Craig, S. L., A remote stereochemical lever arm effect in polymer mechanochemistry. *Journal of the American Chemical Society* **2014,** *136* (43), 15162-15165.
31. Ghanem, M. A.; Basu, A.; Behrou, R.; Boechler, N.; Boydston, A. J.; Craig, S. L.; Lin, Y.; Lynde, B. E.; Nelson, A.; Shen, H.; Storti, D. W., The role of polymer mechanochemistry in responsive materials and additive manufacturing. *Nature Reviews Materials* **2020,** *6* (1), 84-98.
32. Rohde, R. C.; Basu, A.; Okello, L. B.; Barbee, M. H.; Zhang, Y.; Velev, O. D.; Nelson, A.; Craig, S. L., Mechanochromic composite elastomers for additive manufacturing and low strain mechanophore activation. *Polymer Chemistry* **2019,** *10* (44), 5985-5991.
33. Davis, D. A.; Hamilton, A.; Yang, J.; Cremar, L. D.; Van Gough, D.; Potisek, S. L.; Ong, M. T.; Braun, P. V.; Martinez, T. J.; White, S. R.; Moore, J. S.; Sottos, N. R., Force-induced activation of covalent bonds in mechanoresponsive polymeric materials. *Nature* **2009,** *459* (7243), 68-72.
34. Li, Z. a.; Toivola, R.; Ding, F.; Yang, J.; Lai, P. N.; Howie, T.; Georgeson, G.; Jang, S. H.; Li, X.; Flinn, B. D., Highly sensitive built-in strain sensors for polymer composites: Fluorescence turn-on response through mechanochemical activation. *Advanced Materials* **2016,** *28* (31), 6592-6597.

35. Calvino, C.; Guha, A.; Weder, C.; Schrettl, S., Self-Calibrating Mechanochromic Fluorescent Polymers Based on Encapsulated Excimer-Forming Dyes. *Adv Mater* **2018,** *30* (19), e1704603.
36. Grady, M. E.; Beiermann, B. A.; Moore, J. S.; Sottos, N. R., Shockwave loading of mechanochemically active polymer coatings. *ACS Appl Mater Interfaces* **2014,** *6* (8), 5350-5.
37. Karman, M.; Verde-Sesto, E.; Weder, C.; Simon, Y. C., Mechanochemical Fluorescence Switching in Polymers Containing Dithiomaleimide Moieties. *ACS Macro Letters* **2018**, 1099-1104.
38. Peterson, G. I.; Larsen, M. B.; Ganter, M. A.; Storti, D. W.; Boydston, A. J., 3D-printed mechanochromic materials. *ACS applied materials & interfaces* **2015,** *7* (1), 577-583.
39. Piermattei, A.; Karthikeyan, S.; Sijbesma, R. P., Activating catalysts with mechanical force. *Nature chemistry* **2009,** *1* (2), 133-137.
40. Diesendruck, C. E.; Steinberg, B. D.; Sugai, N.; Silberstein, M. N.; Sottos, N. R.; White, S. R.; Braun, P. V.; Moore, J. S., Proton-coupled mechanochemical transduction: a mechanogenerated acid. *Journal of the American Chemical Society* **2012,** *134* (30), 12446-12449.
41. Gunckel, R.; Koo, B.; Xu, Y.; Pauley, B.; Hall, A.; Chattopadhyay, A.; Dai, L. L., Grafted Cinnamoyl-based Mechanophores for Self-Sensing and Photochemical Healing Capabilities in Epoxy. *ACS Applied Polymer Materials* **2020,** *2* (9), 3916-3928.
42. Gossweiler, G. R.; Hewage, G. B.; Soriano, G.; Wang, Q.; Welshofer, G. W.; Zhao, X.; Craig, S. L., Mechanochemical activation of covalent bonds in polymers with full and repeatable macroscopic shape recovery. *ACS Macro Letters* **2014,** *3* (3), 216-219.
43. Robb, M. J.; Moore, J. S., A Retro-Staudinger Cycloaddition: Mechanochemical Cycloelimination of a beta-Lactam Mechanophore. *J Am Chem Soc* **2015,** *137* (34), 10946-9.
44. Diesendruck, C. E.; Peterson, G. I.; Kulik, H. J.; Kaitz, J. A.; Mar, B. D.; May, P. A.; White, S. R.; Martínez, T. J.; Boydston, A. J.; Moore, J. S., Mechanically triggered heterolytic unzipping of a low-ceiling-temperature polymer. *Nature chemistry* **2014,** *6* (7), 623-628.
45. Larsen, M. B.; Boydston, A. J., Successive mechanochemical activation and small molecule release in an elastomeric material. *Journal of the American Chemical Society* **2014,** *136* (4), 1276-1279.
46. Hu, X.; Zeng, T.; Husic, C. C.; Robb, M. J., Mechanically Triggered Small Molecule Release from a Masked Furfuryl Carbonate. *J Am Chem Soc* **2019,** *141* (38), 15018-15023.
47. Sottos, N. R., Polymer mechanochemistry: Flex, release and repeat. *Nat Chem* **2014,** *6* (5), 381-3.
48. Lavalle, P.; Boulmedais, F.; Schaaf, P.; Jierry, L., Soft-mechanochemistry: mechanochemistry inspired by nature. *Langmuir* **2016,** *32* (29), 7265-7276.
49. Wang, L.; Zhou, W.; Tang, Q.; Yang, H.; Zhou, Q.; Zhang, X., Rhodamine-functionalized mechanochromic and mechanofluorescent hydrogels with enhanced mechanoresponsive sensitivity. *Polymers* **2018,** *10* (9), 994.
50. Ballance, W. C.; Seo, Y.; Baek, K.; Chalifoux, M.; Kim, D.; Kong, H., Stretchable, anti-bacterial hydrogel activated by large mechanical deformation. *J Control Release* **2018,** *275*, 1-11.
51. Chen, H.; Yang, F.; Chen, Q.; Zheng, J., A Novel Design of Multi-Mechanoresponsive and Mechanically Strong Hydrogels. *Adv Mater* **2017,** *29* (21).
52. Chen, J.; Peng, Q.; Peng, X.; Han, L.; Wang, X.; Wang, J.; Zeng, H., Recent advances in mechano-responsive hydrogels for biomedical applications. *ACS Applied Polymer Materials* **2020,** *2* (3), 1092-1107.
53. Matsuda, T.; Kawakami, R.; Namba, R.; Nakajima, T.; Gong, J. P., Mechanoresponsive self-growing hydrogels inspired by muscle training. *Science* **2019,** *363* (6426), 504-508.
54. Mier, L. J.; Adam, G.; Kumar, S.; Stauch, T., The Mechanism of Flex-Activation in Mechanophores Revealed By Quantum Chemistry. *ChemPhysChem* **2020,** *21* (21), 2402.
55. Wijnen, J. W.; Engberts, J. B., Retro-Diels− Alder reaction in aqueous solution: toward a better understanding of organic reactivity in water. *The Journal of organic chemistry* **1997,** *62* (7), 2039-2044.
56. van Der Wel, G. K.; Wijnen, J. W.; Engberts, J. B., Solvent Effects on a Diels− Alder Reaction Involving a Cationic Diene: Consequences of the Absence of Hydrogen-Bond Interactions for Accelerations in Aqueous Media. *The Journal of organic chemistry* **1996,** *61* (25), 9001-9005.
57. Stevenson, R.; De Bo, G., Controlling reactivity by geometry in retro-diels–alder reactions under tension. *Journal of the American Chemical Society* **2017,** *139* (46), 16768-16771.
58. Su, X.; Chen, B., Tough, resilient and pH-sensitive interpenetrating polyacrylamide/alginate/montmorillonite nanocomposite hydrogels. *Carbohydr Polym* **2018,** *197*, 497-507.

59. Zhuang, Y.; Yu, F.; Chen, H.; Zheng, J.; Ma, J.; Chen, J., Alginate/graphene double-network nanocomposite hydrogel beads with low-swelling, enhanced mechanical properties, and enhanced adsorption capacity. *Journal of Materials Chemistry A* **2016,** *4* (28), 10885-10892.
60. Novikov, V.; Kuzmin, V.; Kuznetsov, S.; Darvin, M.; Lademann, J.; Sagitova, E.; Ustynyuk, L. Y.; Prokhorov, K.; Nikolaeva, G. Y., DFT study of Raman spectra of polyenes and ß-carotene: Dependence on length of polyene chain and isomer type. *Spectrochimica Acta Part A: Molecular and Biomolecular Spectroscopy* **2021,** *255*, 119668.
61. Sun, J.-Y.; Zhao, X.; Illeperuma, W. R.; Chaudhuri, O.; Oh, K. H.; Mooney, D. J.; Vlassak, J. J.; Suo, Z., Highly stretchable and tough hydrogels. *Nature* **2012,** *489* (7414), 133-136.
62. Buche, M. R.; Silberstein, M. N., Chain breaking in the statistical mechanical constitutive theory of polymer networks. *arXiv preprint arXiv:2104.08866* **2021**.
63. Larsen, M. B.; Boydston, A. J., Successive mechanochemical activation and small molecule release in an elastomeric material. *J Am Chem Soc* **2014,** *136* (4), 1276-9.
64. Li, N.-N.; Zhang, Y.-L.; Mao, S.; Gao, Y.-R.; Guo, D.-D.; Wang, Y.-Q., Palladium-catalyzed C–H homocoupling of furans and thiophenes using oxygen as the oxidant. *Organic letters* **2014,** *16* (10), 2732-2735.
65. Sivanantham, M.; Kesavamoorthy, R.; Sairam, T.; Sabharwal, K.; Raj, B., Stimulus response and molecular structural modification of polyacrylamide gel in nitric acid: A study by Raman, FTIR, and photoluminescence techniques. *Journal of Polymer Science Part B: Polymer Physics* **2008,** *46* (7), 710-720.
66. Levin, I. W.; Harris, W., Interpretation of the vibrational spectra of bicyclic hydrocarbons: norbornane and norbornadiene. *Spectrochimica Acta Part A: Molecular Spectroscopy* **1973,** *29* (10), 1815-1834.
67. Gupta, M. K.; Bansil, R., Laser Raman spectroscopy of polyacrylamide. *Journal of Polymer Science: Polymer Physics Edition* **1981,** *19* (2), 353-360.
68. HORIBA, Raman Spectroscopy for Analysis and Monitoring